OPEN ACCESS Int. J. Phytopathol. 15 (01) 2026. 65-86 DOI: 10.33687/phytopath.015.01.6002

Check for updates

Available Online at EScience Press

International Journal of Phytopathology

ISSN: 2312-9344 (Online), 2313-1241 (Print)

https://esciencepress.net/journals/phytopath

ASSESSING THE *IN VITRO* ANTAGONISTIC POTENTIAL OF INDIGENOUS RHIZOSPHERE BACTERIA AGAINST *FUSARIUM OXYSPORUM*, THE PATHOGEN CAUSING FRUIT ROT ON LIME (*CITRUS LATIFOLIA* (CHRISTM.) SWINGLE)

[a]Nguyen Quoc Khuong, [a]Le Truc Huynh, [b]Nguyen Gia Huy, [a]Tran Trong Khoi Nguyen, [a]Le Thi My Thu, [a]Nguyen Duc Trong, [b]Nguyen Thanh Toan, [a]Le Thanh Quang, [b]Le Thanh Toan, [a]Le Vinh Thuc*

[a] Faculty of Crop Science, College of Agriculture, Can Tho University, Vietnam.

[b] Faculty of Plant Protection, College of Agriculture, Can Tho University, Vietnam.

ARTICLEINFO

Article History

Received: January 21, 2026

Revised: April 11, 2026

Accepted: April 24, 2026

Keywords

β-1,3-glucanase

Chitinase

Fusarium oxysporum

Root-associated bacteria

Siderophores

ABSTRACT

This study was carried out to isolate and characterize rhizosphere bacterial strains with antagonistic activity against *Fusarium* spp., the causal agents of fruit rot in lime (*Citrus latifolia* (Christm.) Swingle) orchards in Can Tho City, Vietnam. A total of 20 rhizosphere soil samples and 20 diseased fruit samples were collected for pathogen and antagonist isolation. Fourteen *Fusarium* spp. isolates were obtained, of which ten were further evaluated for pathogenicity on lime fruits. Strains NBA7 and NBD1 produced typical fruit rot symptoms, with lesion diameters of 3.30 and 2.90 cm, respectively, at 240 h after inoculation, i.e. the pathogen was re-isolated from symptomatic tissues, satisfying Koch's postulates. Based on morphological characteristics and ITS-region sequencing, isolates NBA7 and NBD1 were preliminarily identified as *Fusarium oxysporum*, showing 100% ITS sequence similarity to reference sequences in GenBank. Thirty-nine bacterial strains were isolated from the rhizosphere of lime, and five strains showing strong antagonistic activity against *F. oxysporum* NBA7 (37.3–45.2%) and NBD1 (34.5–63.8%) were selected. These strains were identified by 16S rDNA sequencing as *Bacillus siamensis* CT08 and KS03, *Bacillus velezensis* CT19, *Bacillus aryabhattai* CT11, and *Bacillus amyloliquefaciens* CT10. The selected strains produced chitinase (0.102–0.203 IU/mL), endo-β-1,3-glucanase (0.096–0.392 IU/mL), and exo-β-1,3-glucanase (0.150–0.413 IU/mL), and showed siderophore production ranging from 7.06% to 19.8%. These findings identify indigenous *Bacillus* strains with promising in vitro antagonistic traits and provide a basis for subsequent detached-fruit, greenhouse, and field validation.

Corresponding Author: Le Vinh Thuc

Email: lvthuc@ctu.edu.vn

INTRODUCTION

Citrus crops, belonging to the Rutaceae family, are among the most important fruit crops worldwide and are highly valued for their nutritional potential (Yu *et al*., 2025). Citrus fruits are widely used in various sectors, including healthcare, industry, and food processing (Piattino *et al*., 2024). In Vietnam, citrus cultivation is concentrated in several regions, particularly in the Mekong Delta, where favorable conditions support good adaptation to natural environments (Tran Nguyen *et al*., 2020). Lime is a prominent citrus crop with high agricultural potential in the Mekong Delta. In 2020, lime accounted for 20.2% of the citrus cultivation area and 18.4% of total citrus production in Vietnam (Liem *et al*., 2022).

Despite its economic importance, citrus production is currently facing serious challenges from pests such as insects, nematodes, and especially microbial pathogens that adversely affect crop productivity (Nguyen *et al*.,

2024; Bua *et al*., 2025; Pérez-Hedo *et al*., 2025). Notably, several common diseases have been reported in lime cultivars, including citrus scab caused by *Elsinoe fawcettii* (Pham *et al*., 2025), citrus canker caused by *Xanthomonas citri* (Chen *et al*., 2025), and citrus tristeza virus disease (Sun *et al*., 2024). In particular, lime crops are severely affected by *Fusarium oxysporum* which significantly reduces yield and market value (Hasan *et al*., 2023).

F. oxysporum has been increasingly reported as an important pathogen in citrus production systems in recent years. Typical disease symptoms include soft fruit rot, foul odor, and fruit surface discoloration ranging from yellow to brown, leading to serious losses in yield, postharvest quality, storage, and marketability (Ezrari *et al*., 2022; Hasan *et al*., 2023). Fruit rot caused by *F. oxysporum* adversely affects cultivation and crop management practices, reduces fruit quality, and ultimately decreases yield (Fogliata *et al*., 2013).

In commercial production, chemical fungicides are commonly applied to control fruit rot and other diseases. However, the excessive use of pesticides has resulted in negative impacts on the environment and human health (Zhou *et al*., 2025). As a result, the demand for safe and sustainable biological solutions has increased and become a major priority in modern agriculture (Yildiz *et al*., 2025). Among these approaches, the application of antagonistic microorganisms represents a promising research direction (Monjezi *et al*., 2025).

Rhizosphere bacteria are particularly valued due to their dual role in promoting plant growth and suppressing plant pathogens through mechanisms such as nutrient competition, antibiotic production, and induction of plant resistance (Thepbandit & Athinuwat, 2024; Mon *et al*., 2021). Plant growth–promoting rhizobacteria (PGPR) are recognized as beneficial microorganisms that enhance nutrient availability through both direct and indirect mechanisms. Notably, direct mechanisms include pathogen suppression via the production of siderophores, antimicrobial compounds, and hydrolytic enzymes (Espinosa-Palomeque *et al*., 2025). Through these activities, PGPR can effectively inhibit soilborne and postharvest pathogens, including *Fusarium* species.

Although numerous studies have demonstrated the antagonistic potential of rhizosphere bacteria against *F. oxysporum* in various crops, information regarding rhizosphere bacteria associated with lime and their antagonistic activity against *F. oxysporum* causing fruit rot in the Mekong Delta remains limited. In particular, the diversity of indigenous rhizosphere bacteria and their enzymatic and siderophore-producing abilities have not been sufficiently explored in lime orchards in Can Tho City, Vietnam. Therefore, this study aimed to isolate and identify fungi associated with fruit rot of lime, isolate and identify rhizosphere bacterial strains from lime fields, and evaluate their antagonistic activity against the causal pathogen.

MATERIALS AND METHODS

Duration, Study Site and Materials

The experiment was conducted from October 2024 to December 2025. All experiments were carried out at the Mycology Laboratory, Faculty of Crop Science, College of Agriculture, Can Tho University, Vietnam.

Soil and diseased samples were collected from six citrus-growing households located in Dong Phuoc Commune and Nga Bay Ward, Can Tho City. Potato Dextrose Agar (PDA) medium was prepared for fungal cultivation following Beever and Bollard (1970). King's B liquid and solid media were prepared according to King *et al*. (1954) and used for bacterial isolation and cultivation.

Collection and Isolation of *Fusarium* spp. Samples

Both diseased and healthy lime fruits were collected from multiple locations within Dong Phuoc Commune and Nga Bay Ward, Can Tho City. Diseased samples were selected based on visible disease symptoms from local lime collection center. All samples were placed in nylon bags, transported to the laboratory, and processed following the protocol described by Burgess *et al*. (2009). Briefly, plant tissues were surface-cleaned with 70% ethanol to eliminate epiphytic microorganisms. Small tissue segments were excised from the interface between diseased and healthy tissues, surface-sterilized in 70% ethanol for 3–5 s, air-dried, and then placed onto Petri dishes containing 2% water agar (WA) at five diagonal positions. The plates were incubated at room temperature for 3–5 days. Emerging fungal mycelia were transferred to potato dextrose agar (PDA), and pure cultures were obtained using the single-spore isolation technique as described by Burgess *et al*. (2009). Fungal isolates were coded according to their collection sites, with "NB" representing Nga Bay Ward and "CT" representing Dong Phuoc Commune (formerly Chau Thanh District). The final two digits of each code represented the sequential isolate number.

Pathogenicity of the selected *Fusarium* isolates was confirmed on healthy lime fruits following Koch's

postulates. Healthy fruits were washed, surface-disinfected with 70% ethanol, rinsed with sterile distilled water, and air-dried. Each fruit was wounded using a sterile needle bundle, and a 5-mm-diameter mycelial plug from a 7-day-old *Fusarium* culture grown on PDA was placed on the wound. Sterile PDA plugs were used as the negative control. The inoculated fruits were kept in sterile plastic containers lined with moist sterile filter paper to maintain high humidity and incubated at room temperature. Disease symptoms were observed daily after inoculation. After symptom development, fungal re-isolation was carried out from the lesion margins. Re-isolated colonies were purified and compared with the original isolates based on colony morphology and microscopic characteristics.

Evaluation of the Growth of *Fusarium* spp. Isolates

The experiment was arranged in a completely randomized design (CRD), with each fungal isolate considered as one treatment with three replicates. Each replicate consisted of four independently prepared Petri dishes used as biological replicates. Fungal isolates were inoculated onto PDA medium, and colony growth was evaluated by measuring colony diameter at 48, 96, 120, and 144 hours after inoculation (HAI), following Nguyen *et al*. (2024). Colony growth was calculated using the following formula: $D = (d_1 + d_2)/2$, where d_1 and d_2 represent two perpendicular measurements across the colony. In addition, colony morphology, including mycelial growth pattern and surface and reverse colony coloration, was visually recorded. The mean spore size was determined based on measurements of two perpendicular diagonal axes of the spores (Burgess *et al*., 2009).

Evaluation of the Pathogenicity of *Fusarium* spp. Isolates under Laboratory Conditions

Experimental procedure

The experiment was arranged in a completely randomized design with four independent fruit replicates per fungal isolate. Artificial inoculation was carried out by rinsing healthy fruits with water and disinfecting them with 70% ethanol. Wounds were created at the inoculation sites using a needle bundle, after which 20 µL of sterile distilled water was applied. A 5-mm-diameter fungal mycelial plug from an actively growing culture was placed onto each wound. The inoculated fruits were then placed in containers where high humidity was maintained using filter paper moistened with sterile distilled water (Burgess *et al*., 2009).

Assessment parameter

Lesion diameter (cm) was measured at 3, 5, and 10 days after inoculation (72, 120, and 240 HAI).

Characteristics and morphology of spores

The morphology of spores, including macroconidia, microconidia, conidiophores, and hyphae, was observed. The sizes of macroconidia and microconidia were measured following the criteria described by Nelson (1983). Spore dimensions were measured under a light microscope at 1000× magnification using ToupView software equipped with an ocular micrometer.

Identification of *Fusarium* spp. isolates

Genomic DNA was extracted from fungal mycelia obtained from colonies grown on PDA for 7–10 days. Mycelial samples were transferred into 2.2 mL microcentrifuge tubes, vortexed thoroughly, and incubated at room temperature for 10 min. The samples were then centrifuged at 13,000 rpm for 5 min, and the DNA pellet was washed with 500 µL of 70% ethanol, followed by centrifugation at 13,000 rpm for 5 min and vacuum drying. The DNA was subsequently resuspended in 100 µL of 0.1× TE buffer.

PCR amplification of the ITS region was performed using the primer ITS1 (5′-TCCGTAGGTGAACCTGCGG-3′) and ITS4 (5′-TCCTCCGCTTATTGATATGC-3′) (White *et al*., 1990). Each PCR reaction was carried out in a total volume of 50 µL under the following conditions: initial denaturation at 95°C for 5 min; 30 cycles of denaturation at 95°C for 90 s, annealing at 52°C for 60 s, and extension at 72°C for 90 s; followed by a final hold at room temperature. PCR products were purified and sequenced using an automated DNA sequencer. The obtained sequences were compared with reference sequences in the GenBank database of the National Center for Biotechnology Information (NCBI) using the Basic Local Alignment Search Tool for nucleotides (BLASTN), version 2.14.0 (National Library of Medicine, MD, USA). Multiple sequence alignment was performed using ClustalW algorithm implemented in MEGA version 12 (Molecular Evolutionary Genetics Analysis, PA, USA). Phylogenetic trees were constructed in MEGA 12, with genetic distances calculated using Jukes–Cantor model and tree robustness assessed by bootstrap analysis with 1,000 replicates (Eboigbodin & Biggs, 2008).

Collection and Isolation of Rhizosphere Bacteria with Antagonistic Potential against *Fusarium oxysporum* on Citrus Plants

Rhizosphere soil samples were collected from healthy lime

plants in An Lac Thon Commune, Dong Phuoc Commune, and Nga Bay Ward. Approximately 5 g of soil was collected from the rhizosphere of each plant and transported to the laboratory for processing (Mosca *et al*., 2024). For bacterial isolation, three grams of soil was suspended in 30 mL of distilled water and shaken for 30 min (Abdulkadir & Waliyu, 2012). The suspension was subsequently serially diluted to 10^{-2}, and 20 µL of each dilution was plated onto Petri dishes containing King's B medium, with two plates prepared per sample. The Petri dishes were incubated for 2–3 days, after which single colonies were purified and preserved in glycerol stocks at 4°C.

Screening of Rhizosphere Bacteria with Antagonistic Activity against *Fusarium oxysporum*

Antagonistic activity against *F. oxysporum* was evaluated using a dual-culture assay with four replicates per treatment. A 5-mm-diameter fungal mycelial plug was placed at the center of PDA plates, and bacterial isolates were streaked at three equidistant positions opposite the fungal plug, approximately 1 cm from the edge of the dish (Yoon *et al*., 2012).

Assessment parameters

- Radius of the inhibition zone (RIZ)
- Antagonistic efficiency (AE), calculated using Abbott's formula (1925):

$$GI\ (\%)\ =\ \frac{C-T}{C}\ x\ 100$$

where GI (%) represents antagonistic efficiency; C is the radius of fungal colony growth toward the control side (cm); and T is the radius of fungal colony growth toward the side treated with the antagonistic agent (cm).

Evaluation of the Antagonistic Activity of Rhizosphere Bacterial Isolates against *Fusarium oxysporum* under Laboratory Conditions

Further antagonistic activity assays were conducted in which each treatment consisted of one bacterial isolate with four replicates, each replicate represented by four independently prepared Petri dishes as biological replicates. In the first step, a dual-culture setup was established by placing a 5-mm-diameter fungal mycelial plug at the center of a Petri dish containing PDA medium. Subsequently, sterile filter paper discs (5 mm in diameter) impregnated with bacterial suspensions at a concentration of 10^7 CFU mL^{-1} were placed on the medium, positioned symmetrically on two opposite sides of the fungal plug and approximately 1 cm from the edge of the dish. In some treatments, bacterial inoculum was directly applied by piercing the fungal plug. Distilled water was used as a negative control (Iqbal *et al*., 2024).

Assessment parameters

- Radius of the inner inhibition zone (RIZ)
- Antagonistic efficiency (AE), calculated according to Abbott (1925):

$$GI\ (\%)\ =\ \frac{C-T}{C}\ x\ 100$$

where GI (%) denotes antagonistic efficiency; C is the radius of fungal colony growth toward the control side (cm); and T is the radius of fungal colony growth toward the side treated with the antagonistic agent (cm).

Molecular Identification of Bacterial Isolates with High Antagonistic Potential

The extracted DNA was subjected to PCR amplification of the 16S rRNA gene using primers 8F and 1492R (Turner *et al*., 1999), as described in the iProof™ High-Fidelity PCR Kit protocol (Bio-Rad), and amplified using a T100™ thermal cycler (Bio-Rad, Hercules, CA, USA). PCR product sizes were verified by comparison with a DNA ladder. The PCR products were purified using TIANquick Midi Purification Kit (Tiangen Biotech Ltd., Beijing, China) according to the manufacturer's instructions and re-evaluated for purity by electrophoresis on a 1.0% (w/v) agarose gel. Purified PCR products were sequenced using an automated DNA sequencer at Macrogen DNA Sequencing Service (Macrogen, Seoul, Korea). Sequence chromatograms were analyzed using BioEdit software version 7.0.5.3 (Hall, 1999) and ChromasPro version 1.7. The resulting bacterial sequences were compared with reference sequences available in the GenBank database using Basic Local Alignment Search Tool (BLAST) of the National Center for Biotechnology Information (NCBI) to determine sequence similarity.

Evaluation of the *In Vitro* Antagonistic Potential of Rhizosphere Bacteria

Evaluation of the Production of Degradative Enzymes

Determination of chitinase activity: Chitinase activity was assayed following the method of Bruce *et al*. (1995), based on the amount of reducing sugars released and quantified using the Nelson–Somogyi reagent. Reducing sugars react with copper reagent upon heating to form a brick-red precipitate, which subsequently reacts with the arsenomolybdate reagent to produce a blue color, with absorbance measured at 520 nm. Chitinase activity was also verified by measuring optical density at 490 nm. Chitinase activity was determined by incubating 1 mL of enzyme solution with 1 mL of chitin substrate (1% chitin in acetate buffer, pH 6.0) at 40°C for 60 min. The amount of reducing

sugars released during the reaction was recorded. According to the Nelson method, one unit of enzyme activity (IU mL^{-1}) was defined as the amount of reducing sugar released per minute by 1 mL of enzyme at 40°C and pH 6.0.

Determination of endo-β-1,3-glucanase and exo-β-1,3-glucanase activities:

Enzyme activities were determined according to the method described by Nelson (1944). For each assay, 1 mL of enzyme solution was incubated with 1 mL of carboxymethyl cellulose (CMC; 1% in acetate buffer, pH 5.0) at 40°C for 60 min, after which the amount of glucose released was quantified using the Nelson–Somogyi method. One IU of β-1,3-glucanase activity was defined as the amount of enzyme releasing 1 µmol of glucose equivalent per minute under the assay conditions. Activities were expressed as IU/mL of enzyme solution.

Evaluation of siderophore production

Determination of siderophore activity: The experiment was arranged in a completely randomized design using liquid King's B medium supplemented with siderophore precursors, including 1 g L^{-1} succinate and 0.5 µM $FeCl_3 \cdot 6H_2O$. After 96 h of incubation, the culture broth was centrifuged at 3,500 rpm for 5 min. Subsequently, 1 mL of the supernatant was mixed with 1 mL of the color indicator solution, and absorbance was measured at 630 nm using a spectrophotometer (Schwyn & Neilands, 1987). The color indicator solution consisted of 6 mL of 10 mM hexadecyltrimethylammonium bromide (HDTMA), 1.5 mL of 1 mM $FeCl_3 \cdot 6H_2O$ (prepared in 10 mM HCl), and 7.5 mL of 2 mM chrome azurol S (CAS). In addition, 4.307 g of anhydrous piperazine was added to the mixture, and the pH was adjusted precisely to 5.6. Distilled water was then added, and the solution was mixed thoroughly. Finally, 0.1017 g of 5-sulfosalicylic acid was accurately weighed, dissolved in the solution, mixed well, and brought to a final volume of 100 mL with distilled water in a volumetric flask. Siderophore production was expressed as percent siderophore units (PSU) using the following formula:

$$PSU\ (\%) = [(Ar - As) / Ar] \times 100$$

where: Ar is the absorbance of the reference solution and As is the absorbance of the sample supernatant mixed with CAS reagent. Both absorbance values were measured at 630 nm.

Data Analysis

Data were analyzed using SPSS statistical software version 13.0. Analysis of variance (ANOVA) was performed, and differences among mean values were compared using Duncan's multiple range test at the 5% significance level. Mean values, significance levels, and coefficients of variation (CV) are reported in the tables. Experimental units were independent Petri dishes or fruits, as described above, whereas repeated measurements within a dish or fruit were treated as technical observations and averaged before analysis. Because enzyme and siderophore assays were performed only on the selected strains, these traits were interpreted as associative indicators of potential mechanisms rather than as direct proof of causality.

RESULTS

***Fusarium* spp.**

Collection and isolation of *Fusarium* spp.

Disease symptoms on infected fruits collected from local lime collection center in Dong Phuoc Commune and Nga Bay Ward included large, raised lesions at a single point surrounded by smaller rough protuberances, with pale yellow margins. Additional symptoms included irregular shapes and dark brown to black lesions along the fruit surface, often with lighter centers and light brown margins.

A total of 20 lime fruit samples were collected, from which 14 *Fusarium* spp. isolates causing fruit rot were obtained, including 13 isolates from Nga Bay Ward, Can Tho City and one isolate from Dong Phuoc Commune, Can Tho City. The isolated fungi exhibited relatively similar morphological characteristics and growth characteristics. When cultured on PDA medium at room temperature, colonies grew relatively slowly and completely covered the Petri dishes after approximately 8 days. Colony colors ranged from creamy white to dark purple, light purple, and reddish-orange. The mycelial surface was smooth and closely appressed to the medium, forming concentric rings on the reverse side of the Petri dishes. Some colonies exhibited fine white mycelia, sparse white mycelia, or interwoven white and purple mycelial growth.

Growth ability of *Fusarium* spp.

Colony diameters of the fungal isolates were recorded at different observation times when cultured on PDA medium. At 48 h after inoculation (HAI), the growth of isolates NBA2, NBD1, and NBD7 was relatively high, with colony diameters of 2.57, 2.42, and 2.48 cm, respectively. In contrast, isolates NBA4, NBD8, and NBD9 exhibited the smallest colony diameters at 48 HAI, measuring 1.88, 1.93, and 1.88 cm, respectively. At 96 HAI, colony growth among the isolates was relatively uniform. Isolate NBA2 showed the largest

colony diameter (5.47 cm), whereas isolate NBC9 exhibited the smallest diameter (4.10 cm). The remaining isolates had colony diameters ranging from 4.23 to 5.42 cm. At 120 HAI, isolate NBD6 exhibited the greatest colony diameter (8.18 cm), followed by isolates NBA7 and NBD7, which showed identical diameters of 7.58 cm. Isolate NBD9 had the smallest colony diameter at this time (6.10 cm), while the other isolates ranged from 6.18 to 7.53 cm. At 144 HAI, no substantial differences in colony diameter were observed among most isolates. Isolates CTH3, NBA2, NBA3, NBA3(2), NBA7, NBC7, NBD1, NBD6, NBD8, and NBD9 did not differ significantly, all reaching a colony diameter of 9.00 cm. In contrast, isolate NBC1(1) exhibited the smallest diameter at 144 HAI, measuring 8.07 cm (Table 1).

Table 1. Diameter of the pathogenic fungus (cm) on Petri dishes at different growth stages of *Fusarium oxysporum*.

No.	Isolate's name	Hours after inoculation			
		48	96	120	144
1	CTH3	2.00^{cde}	4.35^{de}	7.01^{d}	9.00^{a}
2	NBA2	2.57^{a}	5.47^{a}	7.33^{c}	9.00^{a}
3	NBA3	2.15^{bc}	4.67^{cd}	7.00^{d}	9.00^{a}
4	NBA3(2)	1.95^{de}	4.92^{bc}	6.48^{f}	9.00^{a}
5	NBA4	1.88^{e}	4.55^{cde}	6.18^{h}	8.67^{b}
6	NBA7	2.23^{b}	5.25^{ab}	7.58^{b}	9.00^{a}
7	NBC1(1)	2.20^{b}	4.73^{cd}	6.25^{gh}	8.07^{c}
8	NBC7	2.23^{b}	5.25^{ab}	7.58^{b}	9.00^{a}
9	NBC9	2.10^{bcd}	4.10^{e}	6.77^{e}	8.08^{c}
10	NBD1	2.42^{a}	5.30^{ab}	7.53^{bc}	9.00^{a}
11	NBD6	2.02^{cde}	5.42^{ab}	8.18^{a}	9.00^{a}
12	NBD7	2.48^{a}	5.32^{ab}	7.58^{b}	8.20^{c}
13	NBD8	1.93^{e}	4.58^{cde}	6.25^{gh}	9.00^{a}
14	NBD9	1.88^{e}	4.23^{de}	6.10^{h}	9.00^{a}
Significance		*	*	*	*
CV (%)		4.03	5.52	1.96	1.06

*Notes: *: Within a column, means followed by different lowercase letters differ significantly at P < 0.05 according to Duncan's multiple range test. * = significant at the 5% level.*

Pathogenicity of *Fusarium* spp. isolates on lime Fruits

At 72 HAI, a total of 80% of the fungal isolates exhibited disease symptoms, characterized by a color change of lime fruits from green to yellow, with brown lesions at the infection sites. Lesion diameters differed among fungal isolates. Notably, isolate NBD6 produced the largest lesion diameter (1.05 cm), whereas isolates CTH3, NBA3(2) and NBD8 exhibited the smallest lesion diameter (0.39-0.44 cm) (Table 2). At 120 HAI, lesions expanded further, and the lime fruits turned uniformly yellow, lesion diameters ranged from 0.53 to 1.64 cm. Among the isolates, NBD1 and NBD6 showed the highest pathogenicity, producing the largest lesion diameter of 1.63-1.64 cm (Table 2). However, by 240 HAI, lesions had enlarged into extensive brown necrotic areas, accompanied by soft rot and the development of white mycelia on the fruit surface. The isolate NBA7 produced the largest lesion diameter (3.30 cm), which was significantly greater than those caused by the remaining isolates NBC7, NBD6, NBA3, NBD1, NBA3(2), NBA2, NBD8, NBD9, and CTH3 (Table 2). In summary, 80% of the *Fusarium* spp. isolates were capable of causing fruit rot in lime, exhibiting typical disease symptoms with varying levels of severity as reflected by lesion diameter. At 240 HAI, isolate NBA7 showed the highest pathogenicity among the 10 isolates evaluated and was therefore selected for subsequent experiments.

Table 2. Diameter of lesions (cm) on fruits at different days after inoculation with *Fusarium oxysporum.*

No.	Isolate's name	Hours after inoculation		
		72	120	240
1	CTH3	0.39^{f}	0.44^{g}	0.65^{g}
2	NBA2	0.69^{d}	0.98^{d}	2.10^{c}
3	NBA3	0.84^{b}	0.84^{c}	1.80^{d}
4	NBA3(2)	0.40^{f}	0.80^{e}	1.10^{f}
5	NBA7	0.74^{c}	1.25^{b}	3.30^{a}
6	NBC7	0.64^{d}	1.08^{c}	1.60^{e}
7	NBD1	0.53^{e}	1.64^{a}	2.90^{b}
8	NBD6	1.05^{a}	1.63^{a}	1.92^{d}
9	NBD8	0.40^{f}	0.53^{f}	0.70^{g}
10	NBD9	0.44^{f}	0.48^{fg}	0.62^{g}
Significance		*	*	*
CV (%)		6.02	4.68	5.50

*Notes: *: Within a column, means followed by different lowercase letters differ significantly at P < 0.05 according to Duncan's multiple range test. * = significant at the 5% level.*

Spore morphology of *Fusarium* spp.

Microscopic observations revealed the presence of chlamydospores, characterized as thick-walled, spherical structures occurring singly or in clusters. In addition to chlamydospores, microconidia were also observed, appearing straight to slightly, oval to elliptical in shape, or nearly straight forms and slightly rounded ends (Figure 1).

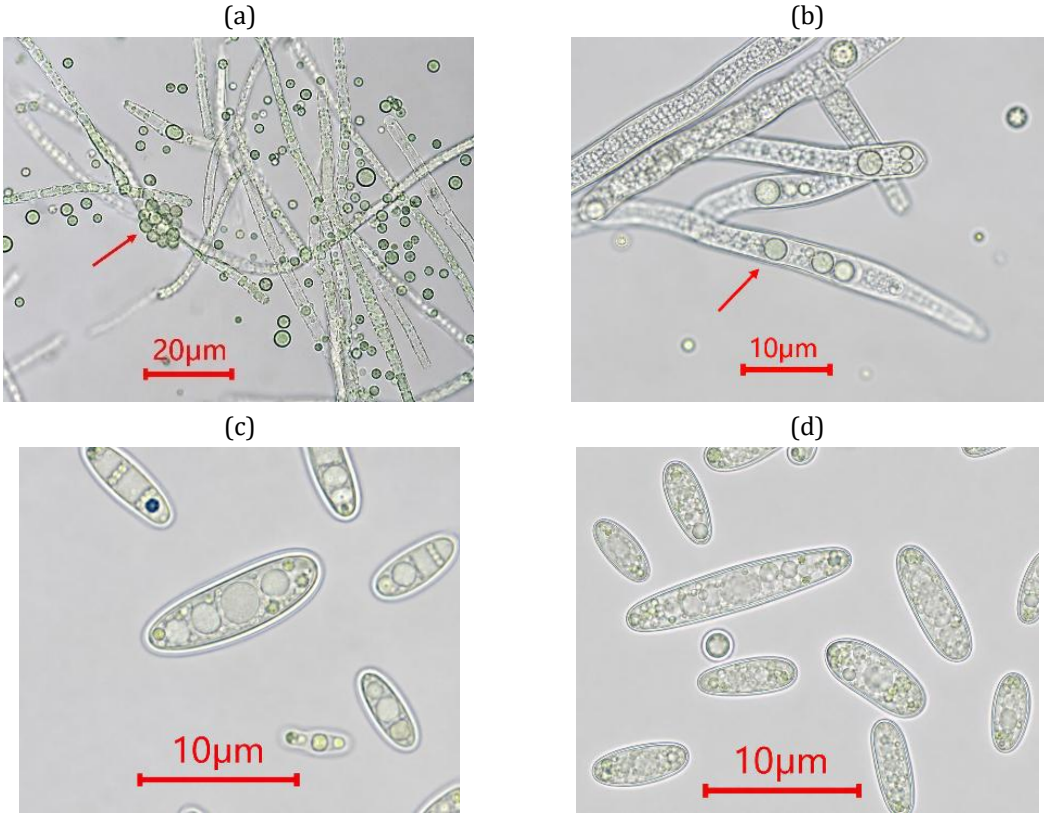

(a) (b) Spores of fungal strain NBA7 after 8 days of incubation; (c) (d) spores of fungal strain NBD1 after 8 days of incubation

Figure 1. Spore morphology of *Fusarium oxysporum*.

Molecular identification of *Fusarium* spp. isolates

Phylogenetic analysis based on the ITS region using the Maximum Likelihood method showed the two fungal isolates, NBA7 and NBD1, clustered with *F. oxysporum* with 100% sequence similarity. Isolate names highlighted in bold represent *F. oxysporum* reference sequences (OM514896; OM514897; PP944822; ON334167). Bootstrap support values from 1,000 replicates are indicated at each node. The scale bar represents 0.01 substitutions per nucleotide position (Figure 2). In addition, these two isolates were clearly differentiated from other species within the genus, such as *F. solani*. The closest related species was *F. proliferatum* (AB106228; AB106224), showing 100% sequence similarity, while a more distant relationship was observed with *Alternaria longipes* (OM398738).

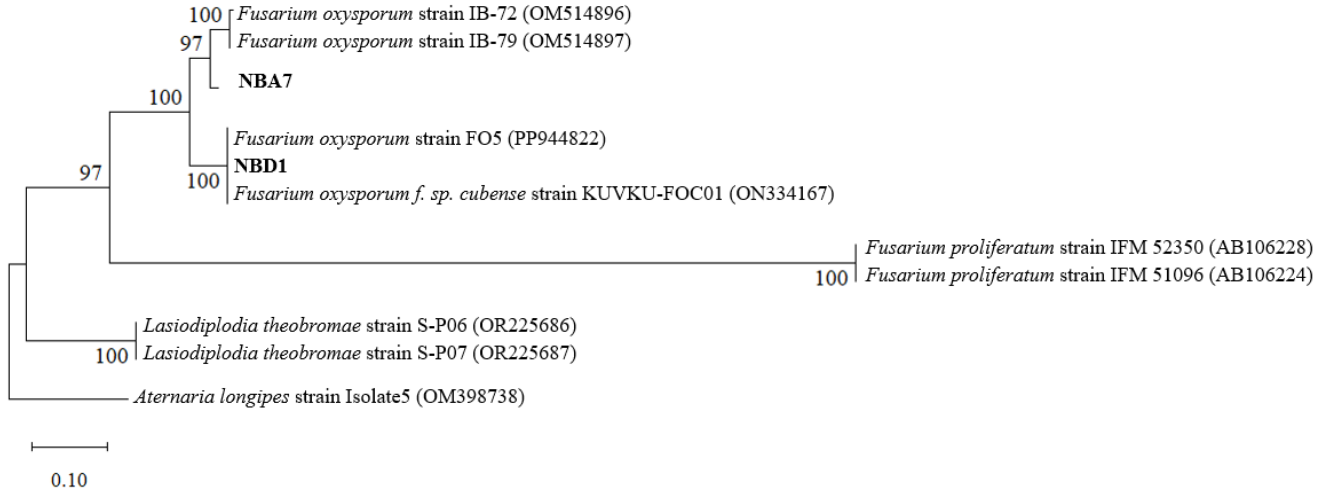

Figure 2. Phylogenetic tree constructed based on ITS sequences of *Fusarium* spp., compared with closely related strains available in the GenBank database. *Note: Accession numbers are shown in parentheses. Alternaria longipes (OM398738) was used as the outgroup.*

Isolation of rhizosphere bacteria

Thirty-nine bacterial strains were isolated from the rhizosphere soil of healthy lime plants. Among them, four strains exhibited *Pseudomonas*-like colonies characterized by opaque, glossy, and smooth morphology. The remaining 35 bacterial isolates formed circular or irregular colonies with dry and wrinkled surfaces, predominantly white to creamy yellow in color, which are characteristic of Gram-positive bacteria.

Screening of rhizosphere bacteria antagonistic to *F. oxysporum*

A total of 39 rhizosphere bacterial strains isolated from lime rhizosphere soil were used to evaluate their inhibitory activity against *F. oxysporum* under in vitro conditions. Fifteen bacterial isolates showed antagonistic activity against *F. oxysporum* and were classified according to inhibition levels as follows: 0–20 (no antagonism, +), 21–49 (moderate antagonism, ++), and ≥50 (strong antagonism, +++) (Table 3). These 15 bacterial isolates were selected for further evaluation of antagonistic activity over time against two selected fungal strains, NBA7 and NBD1 (Figure 3). Following the screening of potential antagonistic bacteria against *F. oxysporum*, the colony morphology of the 15 selected strains grown on King's B agar at 7 DAI was characterized by opaque white, dull, or pale yellow colonies. The colonies exhibited a dry, rough, and uneven surface with dense growth, which is characteristic of Gram-positive bacterial groups (Figure 3).

Table 3. Antagonistic activity of rhizosphere bacteria against the fungal strain *Fusarium oxysporum* NBA7.

No.	Strain name	Hours after inoculation		
		72	96	120
1	CT01	+	+	+
2	CT02	+	+	+
3	CT03	++	++	++
4	CT04	+++	+++	+++
5	CT05	+	+	+
6	CT06	+	+	+
7	CT07	+	+	+
8	CT08	+++	+++	+++
9	CT09	+	+	+
10	CT10	+	+	+
11	CT11	+	+	+
12	CT12	++	++	++
13	CT13	+	+	+
14	CT14	++	++	++
15	CT15	++	++	++
16	CT16	+	+	+
17	CT17	+	+	+
18	CT18	++	++	++
19	CT19	++	++	++
20	CT20	+	+	+
21	CT21	+	+	+
22	CT22	+	+	+
23	CT23	+	+	+
24	KS01	+++	+++	+++
25	KS02	+++	+++	+++
26	KS03	+++	+++	+++
27	KS04	+	+	+
28	NB01	+	+	+
29	NB02	+	+	+
30	NB03	++	++	++
31	NB04	+	+	+
32	NB05	+++	+++	+++
33	NB06	+++	+++	+++
34	NB07	+	+	+
35	NB08	+	+	+
36	NB09	+	+	+
37	NB10	+	+	+
38	NB11	+	+	+
39	NB12	++	++	++

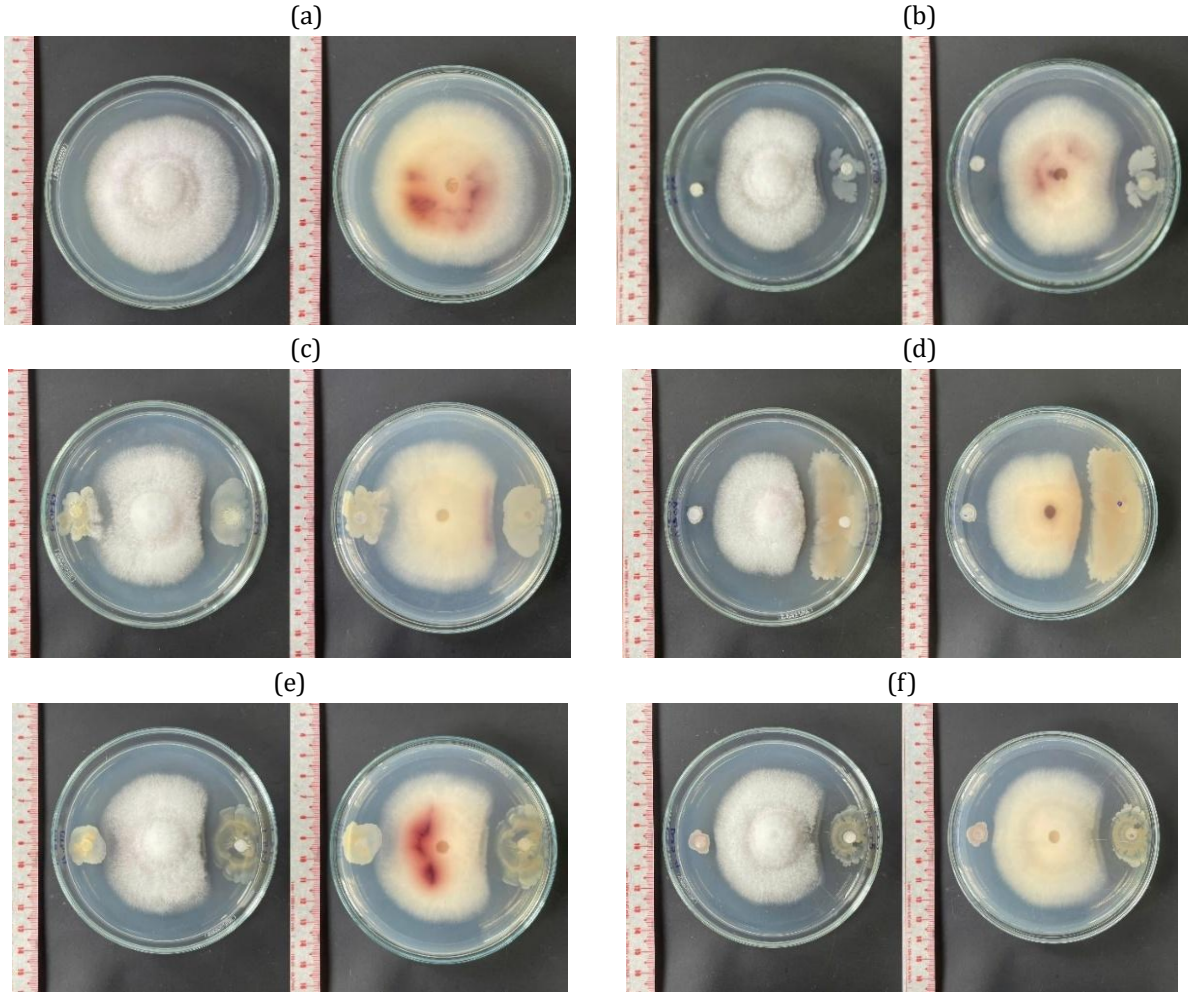

(a) Control (b) NB01 and CT11 (c) CT17 and CT08 (d) KS03 and KS02 (e) CT03 and CT19 (f) NB08 and CT10

Figure 3. Rhizosphere bacterial strains antagonistic to the *Fusarium oxysporum* strain NBA7. Notes: 0–20% = low or no antagonistic activity (+); 21–49% = moderate antagonistic activity (++); ≥50% = strong antagonistic activity (+++).

Antagonistic Activity of Rhizosphere Bacteria against *F. oxysporum* Causing Citrus Fruit Rot using the Dual Culture Method

Antagonistic activity of rhizosphere bacteria against *F. oxysporum* NBD1

Antagonistic efficiency (%): At 72 HAI, the mean antagonistic efficiency (AE) was 9.48%. Among the tested strains, KS03 exhibited the strongest antagonistic activity with an AE of 30.5%. In contrast, strain CT04 did not show any inhibitory ability. The remaining strains showed moderate AE values ranging from 5.00% to 11.4%. At 96 HAI, the mean AE increased to 17.7%. Strain KS03 showed the highest AE (51.1%), which was markedly higher than that of the other strains. Meanwhile, strain CT23 exhibited the lowest AE at this time (9.04%), whereas strain CT04 showed improved growth compared with 72 HAI, indicating the expression of antifungal activity. By 120 HAI, the mean AE reached 24.1%, representing an increase compared with 96 HAI. Antagonistic efficiency differed among the bacterial strains. Strains KS03, CT19, and CT10 exhibited significant inhibition of the fungus, with AE values of 58.1%, 41.4%, and 39.2%, respectively. In contrast, strains CT04, CT23, and NB08 maintained low AE values ranging from 10.8% to 16.7%. At 144 HAI, the mean AE reached its highest level at 30.7%. Strain KS03 maintained the highest antagonistic efficiency (63.8%), followed by strains CT19 (47.4%), CT10 (43.6%), and CT11 (40.2%). Conversely, strains CT04, CT23, and NB08 maintained lower AE levels, ranging from 15.6% to 18.0% (Figure 3; Table 4).

Table 4 Antagonistic efficiency (%) of rhizosphere bacteria against *Fusarium oxysporum* NBD1.

No.	Strain name	Hours after inoculation			
		72	96	120	144
1	CT03	10.5^{bcd}	10.1^{ef}	16.3^{efg}	22.6^{h}
2	CT04	0.0^{e}	13.8^{ef}	15.9^{efg}	15.6^{i}
3	CT08	11.4^{bc}	11.7^{ef}	20.7^{d}	34.5^{ef}
4	CT10	5.71^{cd}	26.2^{c}	39.2^{b}	43.6^{c}
5	CT11	12.1^{b}	19.7^{d}	33.7^{c}	40.2^{cd}
6	CT17	8.57^{bcd}	10.6^{ef}	20.7^{d}	30.5^{g}
7	CT19	11.4^{bc}	31.4^{b}	41.4^{b}	47.4^{b}
8	CT23	6.43^{bcd}	9.04^{f}	10.8^{hi}	18.0^{i}
9	KS02	8.57^{bcd}	11.7^{ef}	16.7^{efg}	32.5^{fg}
10	KS03	30.5^{a}	51.1^{a}	58.1^{ab}	63.8^{a}
11	NB01	10.0^{bcd}	10.6^{ef}	7.37^{i}	11.0^{j}
12	NB02	7.86^{bcd}	14.9^{e}	18.4^{ef}	22.9^{h}
13	NB04	5.00^{de}	10.6^{ef}	15.6^{efg}	24.0^{h}
14	NB05	5.52^{cd}	21.5^{d}	33.9^{c}	37.2^{de}
15	NB08	8.57^{bcd}	12.1^{ef}	13.3^{gh}	16.4^{i}
Average		9.48	17.7	24.1	30.7
Significance		*	*	*	*
CV (%)		38.1	18.3	12.8	8.15

*Note: Within a column, means followed by different lowercase letters differ significantly at P < 0.05 according to Duncan's multiple range test. * = significant at the 5% level.*

Radius of the inhibition zone (RIZ): Across the observation times of 72, 96, 120, and 144 hours after inoculation (HAI), the RIZ values of the 15 rhizosphere bacterial strains ranged from 0.10 to 1.56 cm, reflecting varying levels of pathogen inhibition among the strains (Table 5). At 72 HAI, the highest RIZ was observed in strain NB01 (1.56 cm), followed by strains CT08 and CT11, both with RIZ values of 1.50 cm, indicating strong inhibitory effects. In addition, strain CT17 showed a RIZ of 0.82 cm, whereas strain KS03 exhibited a lower value of 0.35 cm. At 96 HAI, RIZ values ranged from 0.23 to 1.00 cm. Strain NB01 again showed the highest RIZ (1.00 cm), while strain CT17 exhibited the lowest value (0.23 cm). The remaining strains showed RIZ values as follows: CT11 (0.35 cm), CT08 (0.48 cm), CT04 (0.50 cm), CT23 (0.48 cm), NB02 (0.57 cm), NB04 (0.35 cm), KS03 (0.33 cm), KS02 (0.85 cm), CT19 (0.44 cm), CT03 (0.28 cm), CT10 (0.50 cm), NB08 (0.85 cm), and NB05 (0.52 cm). At 120 HAI, three rhizosphere bacterial strains, NB05, CT08, and KS02, maintained stable antagonistic activity, with RIZ values of 0.50 cm, 0.48 cm, and 0.48 cm, respectively. Similarly, strains CT17 and CT03 did not exhibit antagonistic activity at this time point, with RIZ values of 0.00 cm. By 144 HAI, antagonistic activity decreased in most strains. Notably, strain CT08 maintained a relatively high RIZ (0.46 cm), followed by strain KS03 (0.45 cm), indicating continued inhibition of the fungal pathogen. However, several strains, including CT17, CT04, CT23, and NB02, did not show any inhibitory activity. Overall, results recorded from 72 to 144 HAI indicated that strains NB01, CT08, and KS02 consistently exhibited strong antagonistic potential (Figure 4).

Antagonistic activity of rhizosphere bacteria against *F. oxysporum* NBA7

Antagonistic efficiency (%): The antagonistic ability of rhizosphere bacterial strains against *F. oxysporum* NBA7 was evaluated based on antagonistic efficiency (AE) (Table 6). At 72 hours after inoculation (HAI), the mean AE reached 11.9%. The bacterial strains NB05 and KS03 exhibited strong antagonistic activity against *F. oxysporum* NBA7, with AE values ranging from 7.02% to 23.7%. Among them, strain KS03 showed significantly higher antagonistic efficiency compared with the other strains. In addition, several strains such as CT04, CT10, CT08, and CT11 also showed relatively high AE values of 14.9%, 14.9%, 13.2%, and 11.8%, respectively.

Table 5. Radius of the inhibition zone (cm) against *Fusarium oxysporum* NBD1 at different observation times.

No.	Strain name	Hours after inoculation			
		72	96	120	144
1	CT03	0.86^{fg}	0.28^{ef}	0.00^{j}	0.00^{f}
2	CT04	1.19^{c}	0.50^{cd}	0.17^{gh}	0.00^{f}
3	CT08	1.50^{ab}	0.48^{cd}	0.48^{ab}	0.46^{a}
4	CT10	1.05^{de}	0.50^{cd}	0.43^{bc}	0.35^{bc}
5	CT11	1.50^{ab}	0.35^{e}	0.23^{fg}	0.24^{d}
6	CT17	0.82^{g}	0.23^{f}	0.00^{j}	0.00^{f}
7	CT19	0.50^{h}	0.44^{d}	0.29^{ef}	0.38^{b}
8	CT23	1.11^{cd}	0.48^{de}	0.05^{ij}	0.00^{f}
9	KS02	1.44^{b}	0.85^{b}	0.48^{ab}	0.34^{c}
10	KS03	0.35^{i}	0.33^{e}	0.38^{cd}	0.45^{a}
11	NB01	1.56^{a}	1.00^{a}	0.47^{ab}	0.10^{e}
12	NB02	1.13^{cd}	0.57^{c}	0.17^{gh}	0.00^{f}
13	NB04	0.92^{fg}	0.35^{e}	0.10^{hi}	0.00^{f}
14	NB05	0.95^{ef}	0.52^{cd}	0.50^{a}	0.33^{c}
15	NB08	1.48^{ab}	0.85^{b}	0.35^{de}	0.10^{e}
Average		1.09	0.51	0.27	0.18
Significance		*	*	*	*
CV (%)		6.49	11.0	17.6	15.4

*Note: Within a column, means followed by different lowercase letters differ significantly at P < 0.05 according to Duncan's multiple range test. * = significant at the 5% level.*

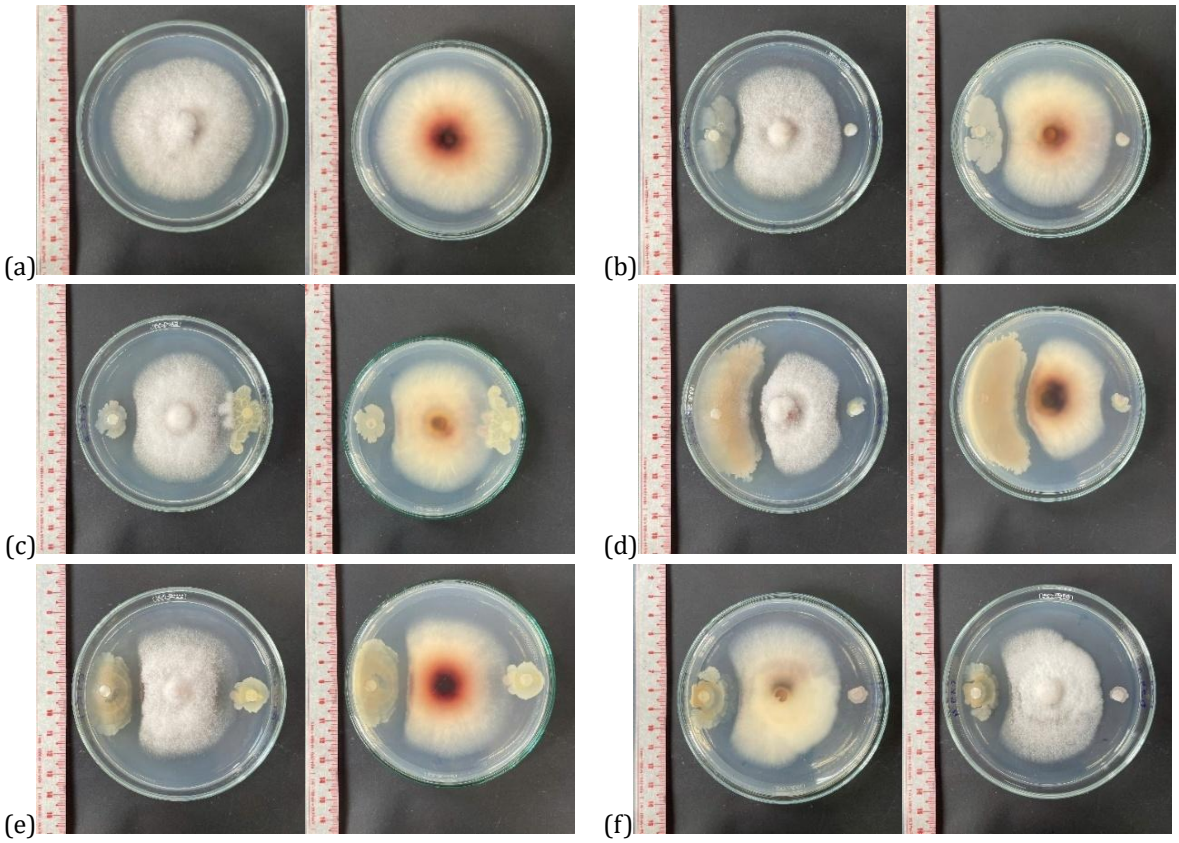

(a)Control (b) CT11 and NB01 (c) CT08 and CT17 (d) KS03 and KS02 (e) CT19 and CT03 (f) CT10 and NB08

Figure 4. Rhizosphere bacterial strains antagonistic to the fungal strain NBD1.

In contrast, strains CT03 and NB05 exhibited the lowest AE at 72 HAI, with values of 7.89% and 7.02%,

respectively. At 96 HAI, the mean AE was 16.9%, indicating that the bacterial strains maintained their inhibitory activity against the pathogen. Strain KS03 showed a markedly higher AE (39.4%) than the remaining strains. Similarly, strains with moderate AE included CT10, CT11, and CT19, with values of 25.0%, 24.6%, and 24.2%, respectively. However, strains CT17 and CT03 maintained low AE levels, ranging from approximately 8.22% to 9.68%. By 120 HAI, the mean AE increased to 21.4%, higher than that at 96 hours. Strain KS03 exhibited the highest AE (47.6%), followed by strains CT11, CT10, CT19, and CT08, with AE values of 36.2%, 35.1%, 33.3%, and 27.4%, respectively. In contrast, strains CT17 (7.10%) and CT23 (9.50%) showed the lowest AE values. At 144 HAI, the mean AE reached 30.7%, the highest among the four observation times. Strain KS03 achieved an AE of 45.2%, maintaining strong antagonistic activity, followed by strain CT11 with 44.0%. Other strains with high activity included CT10 (39.3%), CT19 (37.3%), and CT08 (36.3%), which differed significantly from strains KS03 and CT11. Conversely, strains KS02, CT04, and CT23 exhibited the lowest AE values, at 11.9%, 18.3%, and 19.3%, respectively (Figure 5).

Table 6. Antagonistic efficiency (%) of rhizosphere bacteria against *Fusarium oxysporum* NBA7.

No.	Strain name	Hours after inoculation			
		72	96	120	144
1	CT03	7.89^{ef}	9.68^{de}	11.9^{e}	23.1^{ef}
2	CT04	14.9^{b}	16.2^{c}	10.3^{ef}	18.3^{h}
3	CT08	13.2^{bc}	14.1^{cd}	27.4^{c}	36.3^{bc}
4	CT10	14.9^{b}	25.0^{b}	35.1^{b}	39.3^{b}
5	CT11	11.8^{bcd}	24.6^{b}	36.2^{b}	44.0^{a}
6	CT17	8.22^{def}	8.2^{e}	7.10^{f}	29.8^{d}
7	CT19	11.4^{b-e}	24.2^{b}	33.3^{b}	37.3^{bc}
8	CT23	11.2^{b-e}	11.8^{cde}	9.50^{ef}	19.3^{gh}
9	KS02	9.21^{def}	11.1^{de}	10.1^{ef}	11.9^{j}
10	KS03	23.7^{a}	39.4^{a}	47.6^{a}	45.2^{a}
11	NB01	11.2^{b-e}	15.8^{c}	12.5^{e}	21.9^{fg}
12	NB02	10.5^{c-f}	14.1^{cd}	18.5^{d}	25.7^{e}
13	NB04	9.65^{c-f}	12.6^{cde}	20.8^{d}	34.3^{c}
14	NB05	7.02^{f}	15.9c	21.4^{d}	34.3^{c}
15	NB08	13.2^{bc}	10.4^{de}	19.2^{d}	39.3^{i}
Average		11.9	16.9	21.4	30.7
Significance		*	*	*	*
CV (%)		19.6	16.7	9.81	7.22

*Note: Within a column, means followed by different lowercase letters differ significantly at P < 0.05 according to Duncan's multiple range test. * = significant at the 5% level.*

Inhibition zone (RIZ): The antagonistic ability of rhizosphere bacteria against Fusarium oxysporum NBA7 was also evaluated based on the radius of the inhibition zone (RIZ) (Table 7). At 72 HAI, most strains showed relatively large inhibition zone radii, ranging from 0.37 cm to 1.47 cm. Among them, strains NB01, NB08, and KS02 exhibited high RIZ values of 1.47 cm, 1.42 cm, and 1.36 cm, respectively. In contrast, strains NB02 and KS03 showed lower values of 0.63 cm and 0.37 cm, respectively. The remaining strains ranged from 0.83 cm to 1.10 cm (Table 7). At 96 HAI, strain NB01 maintained a high RIZ value of 1.21 cm, while NB08 reached 0.93 cm, followed by KS02 at 0.83 cm. In contrast, strain CT17 exhibited the lowest value (0.22 cm). Meanwhile, the remaining strains showed moderate values with no marked differences. By 120 HAI, strain NB01 reached 0.70 cm, indicating strong antagonistic activity. This was followed by strains NB05, CT08, and NB08, with RIZ values of 0.50 cm, 0.48 cm, and 0.46 cm, respectively. Conversely, strain CT17 showed a very low RIZ value

(0.10 cm), and strain NB04 did not exhibit clear antagonistic activity. These results indicate that by 120 HAI, variability occurred and some strains no longer showed antagonistic activity. At 144 HAI, three strains showed relatively high RIZ values, including NB05 (0.47 cm), CT10 (0.41 cm), and CT08 (0.41 cm). In contrast, four strains (CT17, CT23, CT03, and NB04) no longer exhibited inhibitory activity. The remaining strains, including CT11, CT04, NB02, KS03, KS02, and CT19, showed RIZ values of 0.31 cm, 0.10 cm, 0.05 cm, 0.23 cm, 0.23 cm, and 0.36 cm, respectively (Figure 5).

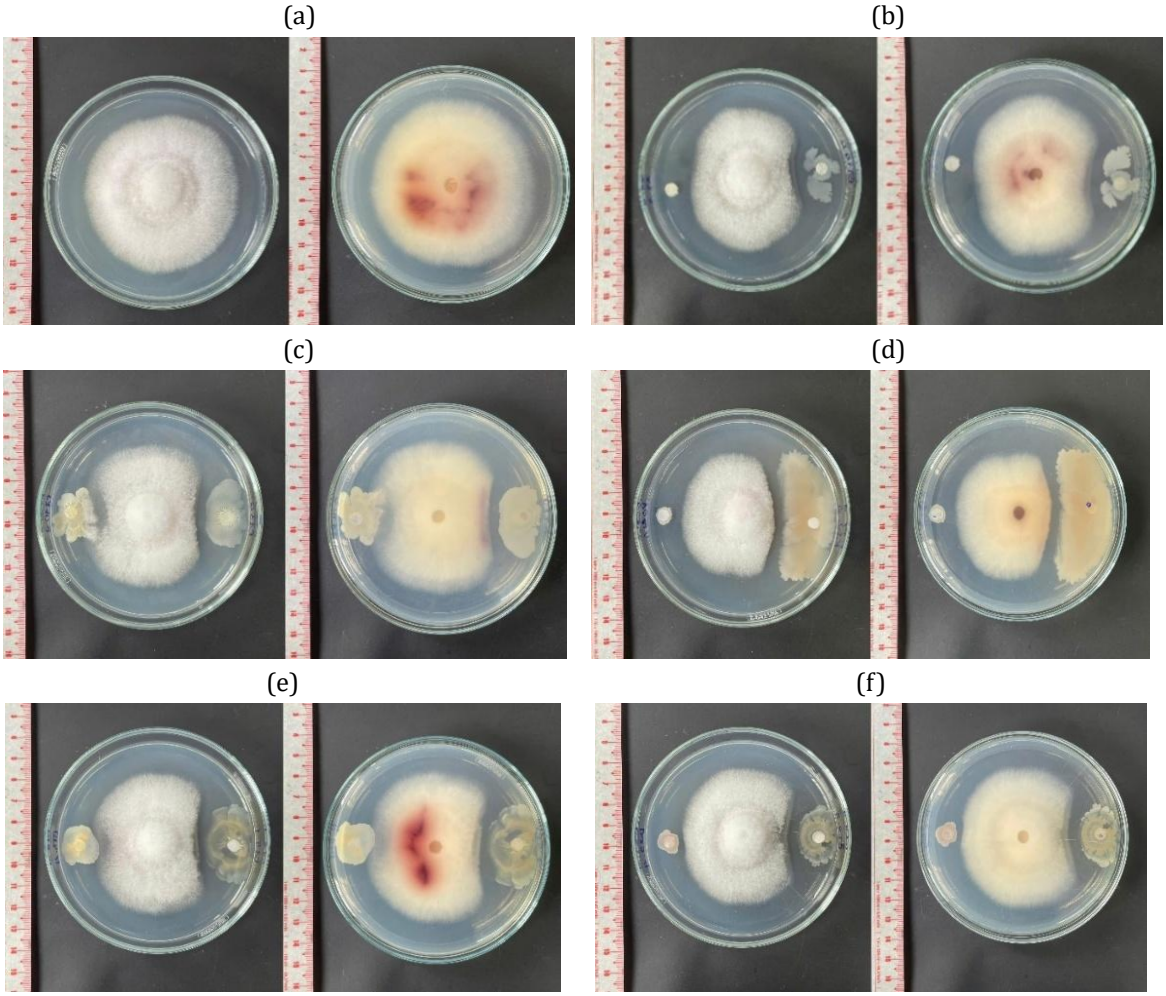

(a) Control (b) NB01 and CT11 (c) CT17 and CT08 (d) KS03 and KS02 (e) CT03 and CT19 (f) NB08 and CT10

Figure 5. Rhizosphere bacterial strains antagonistic to the fungal strain NBA7.

Table 7. Radius of the inhibition zone (cm) against *Fusarium oxysporum* at different observation times.

No.	Strain name	Hours after inoculation			
		72	96	120	144
1	CT03	1.00^{d}	0.43^{hi}	0.15^{f}	0.00^{f}
2	CT04	1.08^{bc}	0.74^{cd}	0.32^{d}	0.10^{e}
3	CT08	1.10^{bc}	0.59^{efg}	0.48^{b}	0.41^{ab}
4	CT10	0.70^{e}	0.59^{efg}	0.46^{b}	0.41^{ab}
5	CT11	0.83^{d}	0.68^{de}	0.40^{c}	0.31^{d}
6	CT17	1.02^{c}	0.22^{j}	0.10^{f}	0.00^{f}
7	CT19	0.69^{e}	0.52^{fgh}	0.38^{cd}	0.36^{bc}

8	CT23	1.13^{b}	0.50^{ghi}	0.13^{f}	0.00^{f}
9	KS02	1.36^{a}	0.83^{bc}	0.33^{d}	0.23^{d}
10	KS03	0.37^{f}	0.38^{i}	0.25^{e}	0.23^{d}
11	NB01	1.47^{a}	1.21^{a}	0.70^{a}	0.40^{b}
12	NB02	0.63^{e}	0.44^{hi}	0.11^{f}	0.05^{ef}
13	NB04	0.73^{de}	0.64^{def}	0.00^{g}	0.00^{f}
14	NB05	0.83^{d}	0.53^{fgh}	0.50^{b}	0.47^{a}
15	NB08	1.42^{a}	0.93^{b}	0.46^{b}	0.20^{d}
Average		0.96	0.61	0.32	0.31
Significance		*	*	*	*
CV (%)		7.78	13.9	13.0	19.1

*Within a column, means followed by different lowercase letters differ significantly at P < 0.05 according to Duncan's multiple range test. * = significant at the 5% level.*

Bacterial isolates selected for molecular identification and biochemical characterization were chosen primarily based on their antagonistic efficiency against both representative *F. oxysporum isolates*, NBA7 and NBD1, particularly at the later observation time of 144 HAI. The radius of the inhibition zone was not used as the sole selection criterion because a large inhibition zone did not always correspond to strong suppression of fungal radial growth; therefore, it was considered as a secondary criterion. Therefore, CT08, KS03, CT19, CT11, and CT10 were selected because they showed relatively consistent antagonistic efficiency against both pathogen isolates and represented promising candidates for further enzymatic and siderophore assays.

Identification of rhizosphere bacterial strains:

Phylogenetic analysis based on the 16S rRNA gene region was performed using the Maximum Likelihood method, in which the names of *Bacillus* strains are shown in bold. Bootstrap percentages from 1,000 replicates are indicated at each node. The scale bar represents 0.02 substitutions per nucleotide site. Strains KS03 and CT08 showed 100% sequence similarity with published sequences of *Bacillus siamensis* (KY962337; KY962331). In addition, strain CT19 exhibited 100% similarity with published sequences of *Bacillus velezensis* (MT436091; MH166800). These results indicate that strain CT19 has potential to antagonize fruit rot disease caused by the fungal pathogen *Fusarium oxysporum*. Furthermore, strain CT11 showed 100% similarity with *Bacillus aryabhattai* sequences (KU161278; KJ206082), with a level of similarity comparable to that of strains KS03, CT08, and CT19. Finally, the 16S rRNA–based phylogenetic tree indicated that strain CT10 had 100% similarity with published sequences of *Bacillus amyloliquefaciens* (OM101144; PQ312879.1; MN176421), suggesting its potential for antagonizing diseases caused by *Fusarium oxysporum* (Figure 6).

Enzyme production and plant growth–promoting activity of selected rhizosphere bacterial strains

Activities of chitinase, endo-β-1,3-glucanase, and exo-β-1,3-glucanase:

Chitinase activity among the rhizosphere bacterial strains ranged from 0.102 to 0.203 IU/mL. Among them, strain CT10 exhibited the highest chitinase activity (0.203 IU/mL), followed by strain CT19 with an activity of 0.102 IU/mL. The remaining three strains, CT11, CT08, and KS03, showed activities ranging from 0.102 to 0.110 IU/mL (Table 8). The highest endo-β-1,3-glucanase activity was observed in strain CT10 (0.392 IU/mL), followed by strain CT11, which showed a lower activity of 0.096 IU/mL. The other three strains, CT19, CT08, and KS03 exhibited activities of 0.110 IU/mL, 0.124 IU/mL, and 0.100 IU/mL, respectively (Table 8).

Exo-β-1,3-glucanase activity differed among the strains, ranging from 0.150 to 0.413 IU/mL. The highest exo-β-1,3-glucanase activity was recorded in strain CT11 (0.413 IU/mL), followed by strains CT10 and CT08 with activities of 0.270 and 0.283 IU/mL, respectively. Next was strain CT19 with an activity of 0.198 IU/mL, while the lowest activity was observed in strain KS03 (0.150 IU/mL) (Table 8). These results indicate that the selected strains differed in putative antifungal traits and may suppress *F. oxysporum* through different mechanisms.

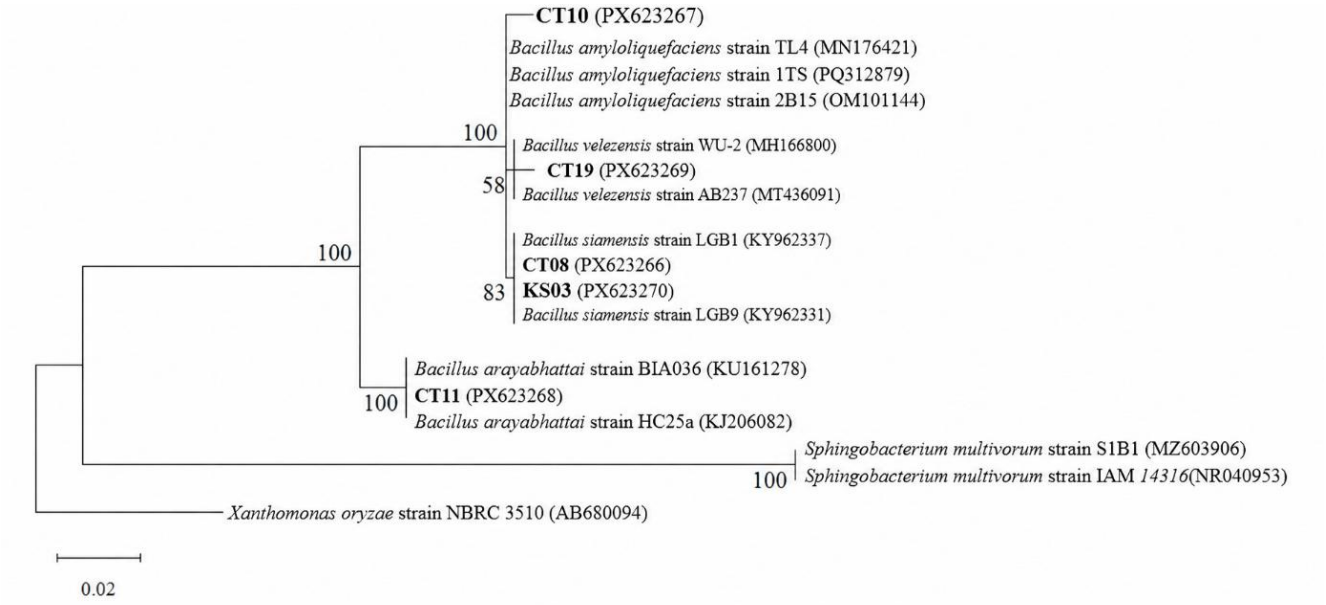

Figure 6. Phylogenetic tree constructed based on 16S rRNA gene sequences of rhizosphere bacteria, compared with closely related strains retrieved from the GenBank database.
Notes: Accession numbers are indicated in parentheses. Xanthomonas oryzae (AB680094) was used as the outgroup strain.

Table 8. Enzyme activities of the selected rhizosphere bacterial strains.

No.	Strain name	Content (IU/mL)		
		Chitinase	Endo- β-1.3 glucanase	Exo-β-1.3 glucanase
1	CT08	0.119^{b}	0.124^{b}	0.283^{b}
2	CT10	0.203^{a}	0.392^{a}	0.270^{b}
3	CT11	0.110^{bc}	0.096^{d}	0.413^{a}
4	CT19	0.102^{d}	0.110^{c}	0.198^{c}
5	KS03	0.113^{bc}	0.100^{cd}	0.150^{d}
Significance		*	*	*
CV (%)		5.20	3.84	3.69

*Within a column, means followed by different lowercase letters differ significantly at P < 0.05 according to Duncan's multiple range test. * = significant at the 5% level.*

Evaluation of siderophore production

The evaluation of siderophore secretion revealed differences among the five bacterial strains. Strain CT19 showed the highest siderophore production (19.8%), followed by strain KS03 with 12.8%. In contrast, strain CT11 exhibited the lowest siderophore-producing ability. The siderophore production of the remaining strains ranged from 7.06% to 10.9%, corresponding to strains CT08, CT11 and CT10, respectively. Overall, siderophore production among the bacterial strains was not markedly different, except for strain CT19, which exhibited notably higher siderophore secretion (Figure 7). The ranking of siderophore production did not completely correspond to the ranking of antagonistic efficiency, suggesting that siderophore-mediated iron competition may contribute to antagonism but is unlikely to be the only mechanism involved.

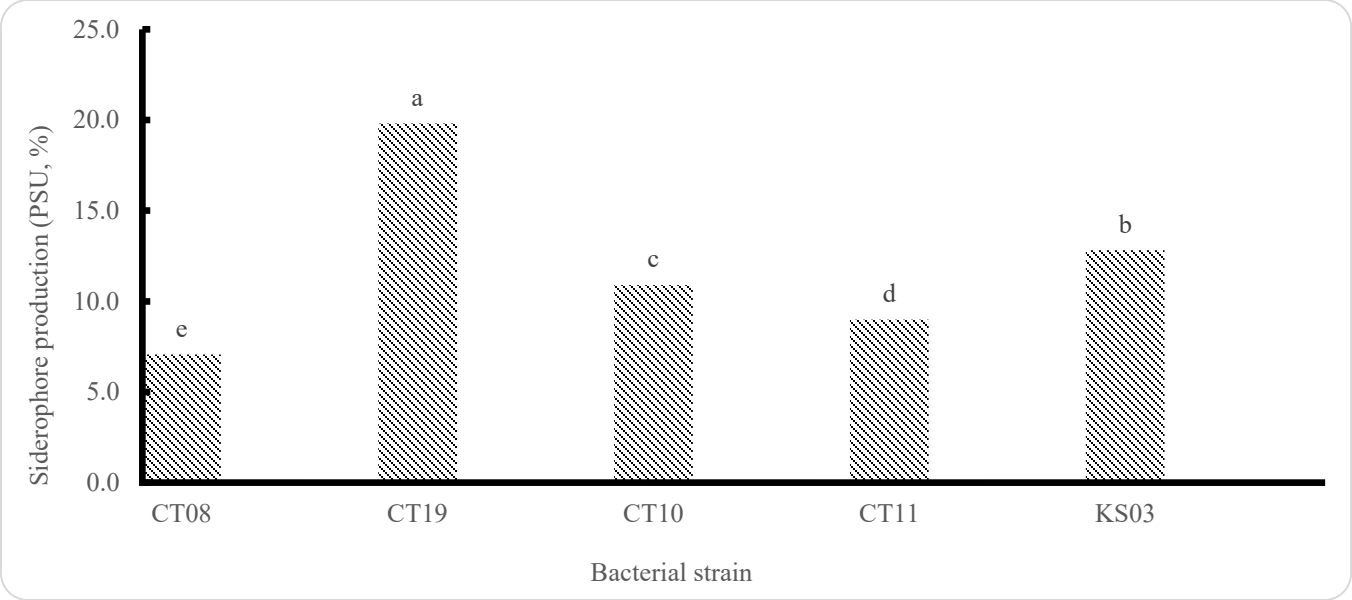

Figure 7. Siderophore production of bacterial strains.

Notes: Columns with the same letters above them are not significantly different at the 5% level according to Duncan's multiple range test.

DISCUSSION

Colonies of *Fusarium* spp. typically display cottony or fluffy mycelial growth with coloration ranging from white to pale purple and forming concentric rings on culture media, with milky-white margins frequently observed (Yang *et al*., 2023). Pigmentation in shades of pink, yellow, or purple is common among *Fusarium* isolates (Ekwomadu & Mwanza, 2023). In citrus, *Fusarium* spp. have been shown to cause fruit rot, with lesion diameters averaging 21.01 ± 2.52 mm under controlled conditions (Yang *et al*., 2023), demonstrating their pathogenic relevance to fruit crops. Microscopic characteristics observed in this study, including sickle-shaped macroconidia and oval microconidia, correspond to previously described morphological traits of *F. oxysporum* (Ajmal *et al*., 2022; Harish *et al*., 2023; Ekwomadu & Mwanza, 2023). Pathogenicity tests on healthy lime fruits produced typical fruit rot symptoms, and the inoculated fungus was re-isolated from symptomatic tissues, supporting Koch's postulates.

In addition, early lesion development may have been influenced by differences in initial pathogen vigor among *Fusarium* isolates. As disease progressed, lesion expansion became more evident, allowing clearer differentiation among isolates. Therefore, the higher variation observed during the early stage should be interpreted as a biological response of the detached-fruit pathogenicity assay rather than as a lack of pathogenic activity.

ITS-based phylogenetic analysis placed the representative pathogenic isolates NBA7 and NBD1 with *F. oxysporum* reference sequences. Indigenous rhizosphere spore-forming *Bacillus* spp., which have strong environmental tolerance and can produce extracellular enzymes, siderophores, and antimicrobial metabolites, may be formulated as cell suspensions or cell-free metabolites for fruit-surface application. However, because the ITS marker has limited discriminatory power within the *Fusarium oxysporum* species complex, the identification should be considered preliminary (Zhang *et al.,* 2026). Additional loci such as TEF-1α (Chen *et al.* 2026), together with broader sampling, will be required to confirm species-level placement and clarify whether the isolates belong to a specific lineage or forma specialis.

Morphological characteristics of rhizosphere bacteria varied among genera, *Pseudomonas* colonies appeared abundant, opaque, shiny, smooth, and convex (Bhuiya *et al*., 2018), while *Bacillus* spp. typically formed large, dry white colonies with irregular, wavy margins (Boottanun *et al*., 2017). Previous studies have demonstrated that *Bacillus* strains can inhibit *Fusarium* species by up to 60% (Chen *et al*., 2025) and suppress *F. oxysporum* isolated from chili pepper through dual-culture assays (Iqbal *et al*.,

2024). In the present study, a total of 39 rhizosphere bacterial isolates were obtained from healthy lime plants. Of these, 15 isolates inhibited *F. oxysporum* in vitro, demonstrating that antagonistic rhizosphere bacteria are indeed present in lime orchards. KS03 consistently showed higher inhibition against pathogen isolates, while CT10, CT11, CT19, and CT08 displayed antagonistic effects at different evaluation times. Therefore, the novelty of the present work is not the discovery of *Bacillus* antagonism in general, but the recovery of indigenous *Bacillus* strains from lime orchards in the Mekong Delta, their evaluation against locally isolated fruit-rot-associated *Fusarium* isolates, and the comparison of multiple antagonistic traits among strains.

Previous reports indicate that *Bacillus amyloliquefaciens* and *Bacillus siamensis* exhibit antifungal activity through the production of hydrolytic enzymes such as chitinase and β-1.3-glucanase (Li *et al*., 2024; Zhang *et al*., 2024), while *B. velezensis* produces β-1.3-glucanase that suppresses phytopathogenic fungi (Vela-Corcia *et al*., 2025). Rhizosphere-derived *Bacillus* isolates have also been associated with enzymatic degradation of fungal cell walls (Rumandani, 2025). In the current study, CT10 expressed relatively high chitinase activity, whereas CT11 revealed stronger β-1.3-glucanase activity, suggesting that enzymatic hydrolysis may contribute to fungal suppression. CT19 produced the highest siderophore levels, indicating that iron competition could be another antagonistic mechanism (Schwyn & Neilands, 1987; Saini *et al*., 2024). These results align with previous observations that antagonistic traits in rhizosphere bacteria are multifactorial and may involve both enzymatic and non-enzymatic pathways. The enzyme and siderophore results provide possible explanations for the observed inhibition but do not prove causality. CT10 showed the highest chitinase and endo-β-1,3-glucanase activities, CT11 produced the highest exo-β-1,3-glucanase activity, and CT19 produced the highest siderophore level. These traits may contribute to degradation of fungal cell-wall components or competition for iron (Terra *et al.*, 2023). However, KS03 showed strong antagonistic efficiency despite only moderate enzyme and siderophore activities, indicating that additional mechanisms, such as lipopeptide antibiotics, volatile compounds, competition for nutrients, or synergistic metabolite production, may also be involved (Li *et al.*, 2022; Al-Mutar et al., 2023; Fan et al., 2025). Thus, the relationship between measured traits and fungal inhibition should be regarded as associative. Future studies should include correlation analyses using a larger set of isolates, cell-free filtrate assays, enzyme-inhibition assays, metabolite profiling, or mutant/knockout approaches to determine which mechanisms are directly responsible for suppression.

Although the antagonistic potential of rhizosphere bacteria has been demonstrated in vitro, further research is needed to determine whether these properties remain stable under environmental conditions encountered in orchards or during postharvest stages. Variations in temperature, humidity, nutrient availability, and microbial community composition may influence antagonistic activity, as suggested by previous studies on fungal suppression in field environments (Khuong *et al*., 2023; Saini *et al*., 2024; Mon *et al*., 2021). Additional work involving metabolite profiling, genomic analyses, and greenhouse or field trials will be required to clarify the reliability of antagonistic traits under practical conditions and to evaluate the feasibility of incorporating these isolates into biological control programs. Nevertheless, this study did not directly test colonization or survival on lime fruit surfaces. Therefore, the present results should be interpreted as a screening step for identifying candidate strains or metabolites, rather than as evidence that rhizosphere bacteria will automatically function on fruit under orchard or postharvest conditions. Moreover, because the ITS region alone has limited resolution for members of the *Fusarium oxysporum* species complex, ITS-based identification was considered preliminary (Zhang *et al.,* 2026). In this study, isolates NBA7 and NBD1 were therefore assigned to *F. oxysporum*/FOSC based on morphology, pathogenicity, and ITS sequence similarity. Further confirmation using more informative loci, such as TEF-1α, RPB1, RPB2, or multilocus sequence analysis, is recommended for precise taxonomic placement.

CONCLUSIONS AND SUGGESTIONS

This study isolated *Fusarium* spp. from lime fruit rot in Can Tho City and showed that representative isolates produced typical symptoms on inoculated fruits, with re-isolation supporting Koch's postulates. Morphology and ITS sequencing supported placement of NBA7 and NBD1 within *F. oxysporum*, although multilocus confirmation is still required. Thirty-nine rhizosphere bacterial isolates were obtained from healthy seedless lime plants, and in vitro screening identified several *Bacillus* strains capable of inhibiting the growth of *F. oxysporum* isolates. Among these, KS03, CT10, CT11, CT19, and CT08 showed the

most relevant antagonistic performance and were identified as *B. siamensis* KS03, *B. amyloliquefaciens* CT10, *B. aryabhattai* CT11, *B. velezensis* CT19, and *B. siamensis* CT08. Enzyme and siderophore assays indicated that the selected strains possess different putative antagonistic traits, but these traits should be interpreted as preliminary mechanistic indicators rather than direct proof of disease control.

Future research should first validate the selected strains in detached-fruit assays, followed by greenhouse, postharvest, and field evaluations under conditions relevant to citrus production. These studies should test fruit-surface colonization, persistence, application timing, formulation stability, compatibility with existing disease-management practices, and effects on fruit quality during storage. Molecular confirmation of *Fusarium* isolates using TEF-1α or multilocus sequencing is also recommended. In addition, metabolite profiling, cell-free culture filtrate assays, and functional validation of enzymes, siderophores, and antimicrobial compounds will be needed before these indigenous *Bacillus* strains can be considered reliable biological control agents for seedless lime fruit rot.

AUTHOR CONTRIBUTIONS

Acknowledgement that all authors accepted the responsibility for the content of the manuscript and consented to its submission, reviewed all the results, and approved the final version of the manuscript. Conceptualization N.Q.K.; methodology N.Q.K., L.V.T., L.T.T; investigation and analysis L.T.H., N.G.H., T.T.K.N., L.T.MT., N.D.T., N.T.T., and L.T.Q.; writing-original draft preparation N.Q.K.; writing-review and editing N.Q.K. and L.V.T.

FUNDING

This research was funded by the Department of Science and Technology of Hau Giang Province through a provincial-level project entitled “Experimental implementation of models to improve and sustainably enhance soil fertility in Hau Giang Province” (2023–2025), under Grant No. 39/HD-KHCN.

REFERENCES

Abdulkadir, M. and S. Waliyu. 2012. Screening and isolation of the soil bacteria for ability to produce antibiotics. European Journal of applied sciences. 4(5): 211-215. DOI: 10.5829/idosi.ejas.2012.4.5.2011.

Ajmal, M., A. Hussain, A. Ali, H. Chen and H. Lin. 2022. Strategies for controlling the sporulation in *Fusarium* spp. Journal of Fungi. 9(1): 10. https://doi.org/10.3390/jof9010010.

Al-Mutar, D. M. K., M. Noman, N. S. A. Alzawar, H. H. Qasim, D. Li and F. Song. 2023. The extracellular lipopeptides and volatile organic compounds of *Bacillus subtilis* DHA41 display broad-spectrum antifungal activity against soil-borne phytopathogenic fungi. Journal of Fungi. 9(8): 797. https://doi.org/10.3390/jof9080797.

Beever, R. E. and E. G. Bollard. 1970. The nature of the stimulation of fungal growth by potato extract. Microbiology. 60(2): 273-279. https://doi.org/10.1099/00221287-60-2-273.

Bhuiya, M., M. K. Sarkar, M. H. Sohag, H. Ali, CK. Roy, L. Akther and A. F. Sarker. 2018. Enumerating antibiotic susceptibility patterns of *Pseudomonas aeruginosa* isolated from different sources in Dhaka City. The Open Microbiology Journal. 12: 172-180. DOI: 10.2174/1874285801812010172.

Boottanun, P. C., C. Potisap, J. G. Hurdle and R. W. Sermswan. 2017. Secondary metabolites from *Bacillus amyloliquefaciens* isolated from soil can kill *Burkholderia pseudomallei*. AMB express. 7(1): 16. DOI: 10.1186/s13568-016-0302-0.

Bruce, A., U. Srinivasan, H. J. Staines and TL. Highley. 1995. Chitinase and laminarinase production in liquid culture by *Trichoderma* spp. and their role in biocontrol of wood decay fungi. International Biodeterioration & Biodegradation. 35(4): 337-353. https://doi.org/10.1016/0964-8305(95)00047-3.

Bua, C., M. C. Tambè, S. C. Taguali, M. Riolo, A. Vitale, A. Pane and SO. Cacciola. 2025. Phytophthora inundata: A new root pathogen of citrus in Europe and the Mediterranean region. Plants. 14(9): 1333. https://doi.org/10.3390/plants14091333.

Burgess, L. W., T. E. Knight, L. Tesoriero and HT. Phan. 2009. Diagnostic manual for plant diseases in Vietnam. ACIAR Monograph No. 129. 210 pp. ACIAR: Canberra.

Chen, X., H. Liu, L. Dong, J. Shi, Z. Ma, L. Yan and Y. Yin. 2025. Identification and characterization of *Fusarium incarnatum* causing leaf spot and fruit rot on luffa in China. *Plants*. 14(6): 845. https://doi.org/10.3390/plants14060845.

Chen, C.C., W. T. Sun, Y. P. Ho, Lin, Y.J. and S.S. Ko. 2026. *Fusarium oxysporum* f. sp. phalaenopsidis, a Novel Forma Specialis Causing Leaf Yellowing of Orchids. Plant Disease. 110(4): 1425–1448. https://doi.org/10.1094/PDIS-11-24-2335-RE

Eboigbodin, K. E. and C. A. Biggs. 2008. Characterization of the extracellular polymeric substances produced by *Escherichia coli* using infrared spectroscopic. proteomic. and aggregation studies. Biomacromolecules. 9(2): 686-695. https://doi.org/10.1021/bm701043c.

Ekwomadu, T. I. and M. Mwanza. 2023. *Fusarium* fungi pathogens. identification. adverse effects. disease management. and global food security: A review of the latest research. Agriculture. 13(9): 1810. https://doi.org/10.3390/agriculture13091810.

Espinosa-Palomeque. B. O. Jiménez-Pérez. RI. Ramírez-Gottfried. P. Preciado-Rangel. A. Buendía-García. GZ. Sifuentes and T. Rivas-García. 2025. Biocontrol of phytopathogens using plant growth promoting rhizobacteria: bibliometric analysis and systematic review. Horticulturae. 11(3): 271. https://doi.org/10.3390/horticulturae11030271.

Ezrari, S., N. Radouane, A. Tahiri, Z. El Housni, F. Mokrini, G. Özer and R. Lahlali. 2022. Dry root rot disease. an emerging threat to citrus industry worldwide under climate change: A review. Physiological and Molecular Plant Pathology. 117: *101753.* https://doi.org/10.1016/j.pmpp.2021.101753.

Fan, H., Q. Wang, J. Bai et al. 2025. Review on the metabolic synergistic mechanisms in fungal-bacterial co-culture systems for VOCs biodegradation: From a microscopic perspective. Reviews in Environmental Science and Bio/Technology. 24: 733-752. https://doi.org/10.1007/s11157-025-09741-7.

Fogliata, G. M., CV. Martínez, M. E. Acosta, M. L. Muñoz and LD. Ploper. 2013. First report of *Fusarium* rot caused by *Fusarium oxysporum* on lemon in Tucumán. Argentina. Plant Disease. 97(7): 989. https://doi.org/10.1094/PDIS-01-12-0069-PDN.

Hall, T. A. 1999. BioEdit: a user-friendly biological sequence alignment editor and analysis program for Windows 95/98/NT. Nucleic Acids Symposium Series. 41: 95-98.

Harish, J., P. P. Jambhulkar, R. Bajpai, M. Arya, P. K. Babele, S. K. Chaturvedi, A. Kumar and DK. Lakshman. 2023. Morphological characterization. pathogenicity screening. and molecular identification of *Fusarium* spp. isolates causing post-flowering stalk rot in maize. Frontiers in Microbiology. 14: 1121781. https://doi.org/10.3389/fmicb.2023.1121781.

Hasan, M. F., M. A. Islam and B. Sikdar. 2023. First report on molecular identification of *Fusarium* species causing fruit rot of mandarin (*Citrus reticulata*) in Bangladesh. F1000Research. 9: 1212. DOI: 10.12688/f1000research.26464.2.

Iqbal, O., R. N. Syed, N. A. Rajput, Y. Wang, A. M. Lodhi, R. Khan, S. M. Jibril, M. Atiq and C. Li. 2024. Antagonistic activity of two *Bacillus* strains against *Fusarium oxysporum* f. sp. *capsici* (FOC-1) causing *Fusarium* wilt and growth promotion activity of chili plant. Frontiers in Microbiology. 15. 1388439. https://doi.org/10.3389/fmicb.2024.1388439.

Khuong, N. Q., D. B. Nhien, L. T. M. Thu, N. D. Trong, P. C. Hiep, V. M. Thuan, L. T. Quang, L. V. Thuc and DT. Xuan. 2023. Using *Trichoderma asperellum* to antagonize *Lasiodiplodia theobromae* causing stem-end rot disease on Pomelo (*Citrus maxima*). Journal of Fungi. 9(10). 981. https://doi.org/10.3390/jof9100981.

King, E. O., M. K. Ward and DE. Raney. 1954. Two simple media for the demonstration of pyocyanin and fluorescin. The Journal of laboratory and clinical medicine. 44(2): 301-307.

Li, J., L. Zhang, G. Yao, L. Zhu, J. Lin, C. Wang, B. Du, Y. Ding and X. Mei. 2022. Synergistic effect of co-culture rhizosphere *Streptomyces*: A promising strategy to enhance antimicrobial activity and plant growth-promoting function. Frontiers in Microbiology. 13: 976484. https://doi.org/10.3389/fmicb.2022.976484.

Li, W. H., Chen, J. Cheng, M. Zhang, Y. Xu, L. Wang and J. Sun. 2024. Improving resistance of mango to *Colletotrichum gloeosporioides* by activating reactive oxygen species and phenylpropane metabolism of *Bacillus amyloliquefaciens* GSBa-1. MetaboliteS. 14(8):417. https://doi.org/10.3390/metabo14080417.

Liem, L. T. T., Y. Tashiro, P. V. T. Tinh and K. Sakai. 2022. Reduction in greenhouse gas emission from lime cultivation using organic fertilizer in a province in Vietnam Mekong Delta region. Sustainability. 14(10): 6102. https://doi.org/10.3390/su14106102.

Mon, Y. Y., S. S. Bidabadi, K. S. Oo and S. J. Zheng. 2021. The antagonistic mechanism of rhizosphere microbes and endophytes on the interaction between banana and *Fusarium oxysporum f. sp. cubense.* Physiological and Molecular Plant Pathology. 116: 101733. https://doi.org/10.1016/j.pmpp.2021.101733.

Monjezi, N., H. R. Eisvand, R. Lee, M. Levi and DL. Smith. 2025. Navigating complex agricultural challenges: harnessing microbial solutions for sustainable growth and resilience. Frontiers in Agronomy. *7:* 1631654.

Mosca, A., G.Dimaria, D. Nicotra, F. Modica, M. E. Massimino, A. F. Catara, G. Scuderi, M. Ruso and V. Catara. 2024. Soil microbial communities in lemon orchards affected by citrus mal secco disease. Genes. 15(7): 824. https://doi.org/10.3390/genes15070824.

Nelson, N. 1944. A photometric adaptation of the Somogyi method for the determination of glucose. J. biol. Chem. 153(2): 375-380.

Nguyen, D. H., T. M. L. Le, H. T. Nguyen, T. D. Nguyen, T. H. Pham, Q. P. Trinh, N. C. Nguyen. 2024. First report of the damaging pest *Meloidogyne enterolobii* parasitizing mulberry (*Morus alba*) in Vietnam. *Plant Disease.* 108(5): 1406*.* https://doi.org/10.1094/PDIS-12-23-2727-PDN.

Pérez-Hedo, M., M. S. Hoddle, F. Alferez, L. Batista, G., A. Beattie, S. Chakravarty and A. Urbaneja. 2025. Global strategies to manage huanglongbing (HLB) and its vectors: insights and implications for the Mediterranean region. *Entomologia Generalis. 45(1): 1-16.* DOI: 10.1127/entomologia/2024/2877.

Pham, N. Q., B. D. Wingfield, I. Barnes, R. Gazis and MJ. Wingfield. 2025. *Elsinoe* species: The rise of scab diseases. Plant Pathology. 74(1): 39-58. https://doi.org/10.1111/ppa.14015.

Piattino, V., D. Aiello, G. Dardani, I. Martino, M. Flores, SG. Aćimović, D. Spadaro, G. Polizzi. and V. Guarnaccia. 2024. *Lasiodiplodia iraniensis* and *Diaporthe* spp. are associated with twig dieback and fruit stem-end rot of sweet orange. *Citrus sinensis*. in Florida. Horticulturae. 10(4): 406. https://doi.org/10.3390/horticulturae10040406.

Rumandani, N. A. 2025. The utilization of *Bacillus* spp. as endophytes in enhancing plant resistance and health against *Fusarium oxysporum*: A Mini Review. Journal of Syntax Literate. 10(1): 490-503. https://doi.org/10.36418/syntax-literate.v10i1.56149.

Saini, N., V. Bundela, S. Singh, M. Sahgal and AV. Singh. 2024. Optimizing Siderophore Production in *Bacillus subtilis* to Enhance Seed Germination and Biocontrol Efficacy against *Alternaria triticina* and *Bipolaris sorokiniana*. Journal of Scientific Research and Reports. 30(8). 313-326. DOI: 10.9734/jsrr/2024/v30i82251.

Schwyn, B. and J. Neilands. 1987. Universal chemical assay for the detection and determination of siderophores. Analytical Biochemistry. 160(1): 47-56. https://doi.org/10.1016/0003-2697(87)90612-9.

Sun, Y., R. K. Yokomi and SY. Folimonova. 2024. *Citrus tristeza virus:* A century-long challenge for the world's citrus industries. Annals of Applied Biology. 185(3): 304-322. https://doi.org/10.1111/aab.12939.

Terra, W. R., C. Ferreira, C. P. Silva. 2023. Plant, Bacterial, and Fungal Cell Wall-Degrading Enzymes. In: Molecular Physiology and Evolution of Insect Digestive Systems. Entomology in Focus, vol 7. Springer, Cham. https://doi.org/10.1007/978-3-031-39233-7_10

Thepbandit, W and D. Athinuwat. 2024. Rhizosphere microorganisms supply availability of soil nutrients and induce plant defense. Microorganisms. 12(3): 558. https://doi.org/10.3390/microorganisms12030558.

Tran Nguyen, T. T., H. H. Le, T. M. H. Ho, T. Dogot, P. Burny, T. N. Bui and P. Lebailly. 2020. Efficiency analysis of the progress of orange farms in Tuyen Quang province. Vietnam towards sustainable development. Sustainability. 12(8). 3170*.* https://doi.org/10.3390/su12083170.

Turner, J.T. and P.A. Backman., 1999. Factors relating to peanut yield increases a er seed treatment with *Bacillus subtilis*. Plant Disease. 75: 347-353. DOI: 10.1094/PD-75-0347.

Vela-Corcia, D., AM. Colino-Palomino, A. de Vicente, A. Pérez García and D. Romero. 2025. Characterization of bvlzgluc. a novel antifungal β-glucanase from *Bacillus velezensis*. with potential agricultural and industrial applications. bioRxiv. 2025-01.

https://doi.org/10.1101/2025.01.23.634490.

Yang, X. Z., Y. B. Wang, S. C. Li, F. Wu, ZY. Luo, J. Y. Chen, M. L. Xiang and M. Chen. 2023. First report of *Fusarium tricinctum* causing fruit rot on navel orange (*Citrus sinensis*) in China. *Plant Disease*. *107(2): 567.* https://doi.org/10.1094/PDIS-04-22-0891-PDN.

Yildiz. MG. G. Romanazzi and MC. Oguz. 2025. Bio-based strategies for biotic and abiotic stress management in sustainable agriculture. *Frontiers in Plant Science*. *15:* 1536460. https://doi.org/10.3389/fpls.2024.1536460.

Yoon, G. Y., Y. S. Lee, S. Y. Lee, R. D. Park, H. N. Hyun, Y. Nam and KY. Kim. 2012. Effects on *Meloidogyne incognita* of chitinase. glucanase and a secondary metabolite from *Streptomyces* cacaoi GY525. Nematology. 14(2): 175-184. DOI: 10.1163/138855411x584124.

Yu, K., M. Zhong, W. Zhu, A. Rashid, R. Han, M. S. Virk and X. Ren. 2025. Advances in computer vision and spectroscopy techniques for non-destructive quality assessment of citrus fruits: A comprehensive review. Foods. 14(3): 386. https://doi.org/10.3390/foods14030386.

Zhang, M., X. Li, Y. Pan, D. Qi, D. Zhou, Y. Chen, J. Feng, Y. Wei, Y. Zhao, K. Li, W. Wang, L. Zhang and J. Xie. 2024. Biocontrol mechanism of *Bacillus siamensis* sp. QN2MO-1 against tomato fusarium wilt disease during fruit postharvest and planting. Microbiological Research. 283: 127694. https://doi.org/10.1016/j.micres.2024.127694.

Zhang, Q., Hyde, K. D., Sun, Y.-R., Zeng, S.-X., Long, H., Bhunjun, C. S., Al-Otibi, F., Li, C., Wang, Y., Liu, F.-Q., & Maharachchikumbura, S. S. N. 2026. Genome-scale phylogenetics and integrative species delimitation to clarify taxonomic boundaries in pestalotiopsis-like fungi. Fungal Diversity. 136: 136003. https://doi.org/10.65390/fdiv.2026.136003.

Zhou, W., M. Li and V. Achal. 2025. A comprehensive review on environmental and human health impacts of chemical pesticide usage. Emerging Contaminants. 11(1): 100410. https://doi.org/10.1016/j.emcon.2024.100410.